Journal of Coordination Chemistry

ISSN: 0095-8972 (Print) 1029-0389 (Online) Journal homepage: http://www.tandfonline.com/loi/gcoo20

Synthesis, spectral, and magnetic studies of benzothiazolium tetrachlorocuprate salts: crystal structure and semiconducting behavior of bis[2-(4-methoxyphenyl)benzothiazolium] tetrachlorocuprate(II)

A. Sarau Devi, Reena Ravindran, Shiji Fazil & R. Minitha

To cite this article: A. Sarau Devi, Reena Ravindran, Shiji Fazil & R. Minitha (2015) Synthesis, spectral, and magnetic studies of benzothiazolium tetrachlorocuprate salts: crystal structure and semiconducting behavior of bis[2-(4-methoxyphenyl)benzothiazolium] tetrachlorocuprate(II), Journal of Coordination Chemistry, 68:13, 2253-2270, DOI: 10.1080/00958972.2015.1042874

To link to this article: http://dx.doi.org/10.1080/00958972.2015.1042874

Journal of Coordination Chemistry, 2015
Vol. 68, No. 13, 2253–2270, http://dx.doi.org/10.1080/00958972.2015.1042874

Synthesis, spectral, and magnetic studies of benzothiazolium tetrachlorocuprate salts: crystal structure and semiconducting behavior of bis[2-(4-methoxyphenyl)benzothiazolium] tetrachlorocuprate(II)

A. SARAU DEVI*†, REENA RAVINDRAN‡, SHIJI FAZIL§ and R. MINITHA¶

†Department of Chemistry, Fatima Mata National College, Kollam, India
‡Department of Chemistry, Sree Narayana College, Thiruvananthapuram, India
§Department of Chemistry, Mannaniya College of Arts and Science, Thiruvananthapuram, India
¶Department of Chemistry, S.N. College, Kollam, India

(*Received 8 November 2014; accepted 1 April 2015*)

$$2\,C_{14}H_{11}NOS + Cu^{2+} + 4HCl \xrightarrow[\Delta]{MeOH} (C_{14}H_{12}NOS)_2CuCl_4 + 2H^+$$

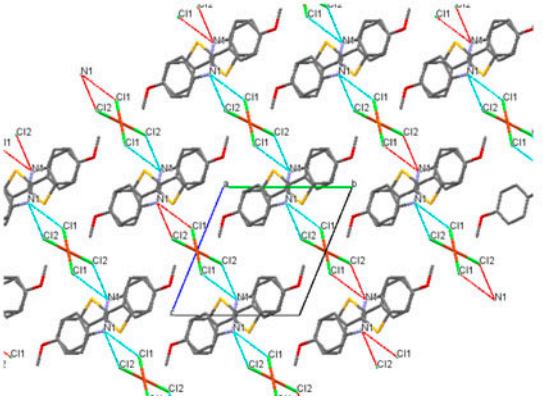

Reaction of $Cu(NO_3)_2{\cdot}3H_2O$ with substituted 2-phenylbenzothiazoles and HCl in methanolic solution gave $(2\text{-PBZ})_2[CuCl_4]$, [2-PBZ = substituted 2-phenyl benzothiazolium]. Three such compounds, 2-(4-methoxyphenyl) benzothiazolium tetrachlorocuprate(II), $[(mpbH)_2CuCl_4]$, $(C_{14}H_{12}NSO)_2CuCl_4$; 2-(3-methoxy-4-hydroxyphenyl) benzothiazolium tetrachlorocuprate(II), $[(mhpbH)_2CuCl_4]$ $(C_{14}H_{12}NSO_2)_2CuCl_4$ and 2-(2-hydroxyphenyl)benzothiazolium tetrachlorocuprate(II), $[(hpbH)_2CuCl_4]$ $(C_{13}H_9NSO)_2CuCl_4$ were isolated and characterized by spectral and thermal studies. Single crystal analysis of bis[2-(4-methoxyphenyl) benzothiazolium] tetrachlorocuprate(II) $[(mpbH)_2CuCl_4]$ reveals that it crystallizes in P-1 space group with square planar $CuCl_4^{2-}$ and almost planar 2-(4- methoxyphenyl)benzothiazolium cation ($mpbH^+$). The discrete $CuCl_4^{2-}$ units are held between layers of 2-(4-methoxyphenyl) benzothiazolium, ($mpbH^+$) units, mainly by ionic and hydrogen bonding, resulting in a 3-D crystal lattice. This compound exhibits green-to-yellow

*Corresponding author. Email: sarayu@fatimacollege.net

thermochromic transformation on heating. The variable-temperature magnetic susceptibility measurements of all the compounds show normal paramagnetic behavior with no significant interactions between the paramagnetic Cu(II) centers. The electrical conductivity for crystal salts of $[(mpbH)_2CuCl_4]$ was 1.99×10^{-4} S cm^{-1} at room temperature indicating a semiconductor.

Keywords: Crystal structure; Benzothiazolium tetrachlorocuprate(II); Magnetic susceptibility; Thermochromism; Semiconductor

1. Introduction

Benzothiazoles are of interest due to their potential pharmacological properties such as anticancer, antimicrobial, photosensitizing, antidiabetic, antioxidant, and HIV inhibiting activities [1–6]. The extensive biological activity of benzothiazole derivatives are attributed primarily to the presence of extended π-delocalized systems, capable of binding to DNA via π–π interactions [7]; a large number of therapeutic agents are synthesized with the help of the benzothiazole nucleus [8]. Depending on the efficiency of the chromophore in the aryl system, some benzothiazole derivatives have interesting luminescence [9] or fluorescence properties. Fluorescence and UV–visible properties of benzothiazole complexes are controlled by mode of coordination, as the N- and S-coordinating sites are on different sides of the heterocyclic ring. Soft metal ions will preferentially bind to the S-coordinating site, while hard ions will prefer the N-coordinating site [10]. Benzothiazole-based metal complexes of Re and Tc are also excellent cancer radiopharmaceuticals [11].

Recent developments in inorganic–organic hybrid compounds led us to prepare a series of substituted 2-phenyl benzothiazoles, $A_2[MX_4]$, where A is an organic cation, M is a transition metal ion, and X is a halide [12, 13]. These compounds sometimes exhibit low-dimensional antiferromagnetic exchange interactions [14, 15]. The π/d-cooperative molecular systems involving conducting π electrons of radical cation salts with copper counter anion of localized d spins, attain interest due to its electrical conduction/magnetic properties [16, 17]. Some TTF frameworks, with a backbone of π-conjugated cation radical salt, were reported as organic semiconductors [18]. In some other cases, organic salts possess low-dimensional magnetic moments, because of structural phase transitions due to rotation of $CuCl_4^{2-}$ about crystallographic axes mediated by organic cations [19]. In general, the structures of these compounds can be described as cationic–anionic layers interconnected by ionic interaction, hydrogen bonding, π–anion, and π–π stacking interactions, which play a role in building the entire structure in a 3-D crystal lattice and are responsible for the properties [20, 21]. Here, due to the presence of an active Jahn–Teller effect in Cu(II), the $CuCl_4^{2-}$ species in these compounds becomes stereochemically non-rigid. The geometry usually varies from distorted tetrahedral with D_{2d} symmetry to centrosymmetric square planar with D_{4h} symmetry [22, 23]. The colors of these compounds also depend on geometry, with green observed when the trans Cl–Cu–Cl angle is 180º as in square planar complexes and orange to yellow when the angle decreases. Thus, on application of temperature, most of these compounds exhibit thermochromism due to a possible change on the trans angle along with a change in the entire hydrogen bonding network in the crystal structure [24]. This work deals with the synthesis of a series of substituted 2-phenylbenzothiazole (figure 1) salts with $CuCl_4^{2-}$, the structures of which were proved by various spectral techniques like infrared, electronic, NMR, and ESR, along with thermogravimetric studies.

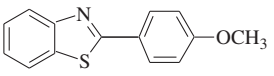

2-(4-methoxyphenyl)benzothiazole, mpb

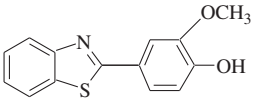

2-(3-methoxy-4-hydroxyphenyl)benzothiazole, mhpb

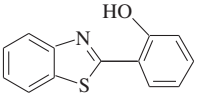

2-(2-hydroxyphenyl)benzothiazole, hpbH

Figure 1. Structures of substituted 2-phenylbenzothiazoles: mpb, mhpb, and hpbH.

The magnetic properties of the $CuCl_4^{2-}$ salts are discussed. The crystal structure of $[(mpbH)_2CuCl_4]$ is discussed, which explains various interactions between cationic and anionic units. The semiconducting behavior of the crystalline compound has been explored.

2. Experimental

$Cu(NO_3)_2{\cdot}3H_2O$, o-aminothiophenol, anisaldehyde, salicylaldehyde, vanillin, and sodium bisulfite of Analar grade were purchased from Merck and used as received for preparing benzothiazole ligands. Methanol (Merck) was used without purification.

2.1. *Materials and methods*

All chemicals used were Analar, or of high grade. All organic compounds were prepared by literature methods [25]. Elemental analyses were performed on a Vario EL III CHNS analyzer. Infrared spectra were recorded on a Thermo Nicolet AVATAR 370 DTGS model FT-IR Spectrometer using KBr pellets from 4000 to 400 cm^{-1}. The thermal analysis (TGA) was carried out in air with a heating rate of 10 °C min^{-1} using a Perkin Elmer Diamond TG/DTG analyzer. Electronic spectra were recorded in acetonitrile solutions on a Spectro UV–vis Double Beam UVD-3500 Spectrophotometer from 200 to 1500 nm. EPR spectra in the solid state and in acetonitrile at liquid nitrogen temperature were recorded on a Varian E-112 spectrometer with X-band, using TCNE as standard with 100 kHz modulation frequency and 9.1 GHz microwave frequency at SAIF, IIT, Bombay. The DART-mass spectra of the compounds were recorded on a Jeol AccuTOF DART JMS-T100LC mass spectrometer having time-of-flight (TOF) mass analyzer and Direct Analysis in Real Time (DART) source. Magnetic susceptibility data were measured on a Lake Shore Cryotronics, Inc. Vibrating Sample Magnetometer. The electrical conductivity has been measured using a Keithley 2182 A nanovoltmeter for probe conductivity meter (6221 dc current source).

2.2. *X-ray crystallography*

Single crystal of $(mpbH)_2CuCl_4$ (green) of dimensions $0.30 \times 0.20 \times 0.20$ mm was selected and mounted on a Bruker axs Kappa apex 2 CCD diffractometer, equipped with a graphite crystal incident beam monochromator and a fine focus sealed tube Mo Kα ($\lambda = 0.71073$)

X-ray source. The unit cell dimensions and intensity data were recorded at 293 K. The program SAINT/XPREP was used for data reduction and APEX2/SAINT for cell refinement [26]. The structure was solved using SIR92 [27], and refinement was carried out by full-matrix least squares on F^2 using SHELXL-97 [28]. Molecular graphics employed were ORTEP-III [29] and MERCURY 2.4 [30]. The positional parameters for the N–H hydrogen were refined using the riding model.

2.3. *Synthesis of substituted 2-phenylbenzothiazole ligands (mpb, mhpb, and hpbH)*

Equimolar mixture of $NaHSO_3$ (1.25 g, 0.012 mol) and corresponding aldehyde, *viz*. anisaldehyde (1.63 g, 0.012 mol) for mpb, vanillin (1.82 g, 0.012 mol) for mhpb, and salicylaldehyde (1.47 g, 0.012 mol) for hpbH, were refluxed in ethanol (15 mL) for 15–20 min. To the mixture o-aminothiophenol (1.25 g, 0.01 mol) was added and continued to reflux for 4–5 h. On slow cooling, colorless crystalline compound formed in each case was filtered, washed with water, recrystallized from ethanol, and dried over fused $CaCl_2$. The solids were recrystallised from hot ethanol (scheme 1).

mpb: Yield: 86%. M.P.: 110 °C. Color: Colorless. Anal. Found (Calcd for $C_{14}H_{11}NOS$, 241): C, 69.51 (69.68); H, 4.75 (4.59); N, 5.63 (5.80); S, 13.42 (13.28).

mhpb: Yield: 85%. M.P.: 171 °C. Color: Colorless. Anal. Found (Calcd for $C_{14}H_{11}NO_2S$, 257): C, 65.42 (65.27); H, 4.21 (4.30); N, 5.62 (5.44); S, 12.63 (12.46).

hpbH: Yield: 82%. M.P.: 129 °C. Color: Colorless. Anal. Found (Calcd for $C_{13}H_9NOS$, 227): C, 68.75 (68.69); H, 3.76 (3.99); N, 6.32 (6.16); S, 14.28 (14.10).

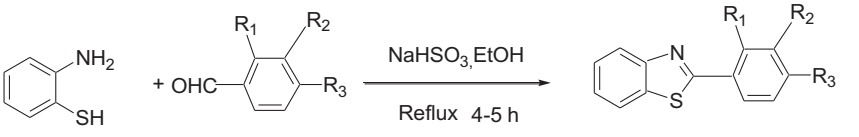

R_1= H, R_2 = H, R_3 = OCH_3 for mpb

R_1= H, R_2 = OCH_3, R_3 = OH for mhpb

R_1= OH, R_2 = H, R_3 = H for hpbH

Scheme 1. Synthesis of substituted 2- phenyl benzothiazoles.

2.4. *Spectral characterization of mpb, mhpb, and hpbH*

2.4.1. Infrared spectra. Bands in the 1625–1300 cm^{-1} range are due to overall ring skeletal (benzene and thiazole ring) stretching mode [31, 32]. The characteristic $\nu_{(C=N)}$ vibrations of thiazole for mpb, mhpb, and hpbH are assigned at 1597, 1592, and 1588 cm^{-1}, respectively, and $\nu_{(C-S)}$ at 687, 716, and 700 cm^{-1}, respectively [33]. Bands at 1308–962 cm^{-1} correspond to the CH– in plane deformation of benzene and thiazole rings while out of plane deformations are observed at 860–716 cm^{-1}. The $\nu_{(O-H)}$ of mhpb appeared as a broad band at 3200–2800 cm^{-1} while $\nu_{(O-H)}$ of hpbH appeared as a weak peak at 3057 cm^{-1}. The phenolic C–O stretch for mhpb is observed at 1191 cm^{-1} and the same for hpbH is at 1219 cm^{-1}. The O–CH_3 stretching mode for mpb and mhpb is ascribed

to peaks at 1021 and 1007 cm^{-1} while bending mode to the peaks at 434 and 438 cm^{-1}, respectively [34].

2.4.2. ^{1}H NMR spectra. In the ligands, signals between 6.9 and 8.1 ppm are assigned to aromatic protons of both benzothiazole and phenyl ring [35]. Comparison of the chemical shift of the protons in the phenyl ring shows very similar values for mpb, mhpb, and hpbH.

Due to the presence of an additional OH and subsequent establishment of hydrogen bonding in mhpb, the chemical shift values of the protons in the substituted 2- phenyl rings show slight variation in comparison with those of mpb. The methoxy protons of mpb resonate at 3.87 ppm. The doublet at 8.03 ppm corresponds to C(9)H and C(13)H, whereas the doublet at 6.99 ppm is due to C(10)H and C(12)H in mpb.

In mhpb, the $–OCH_3$ protons show a slight downward shift to 4.01 ppm due to the withdrawal of electron density by adjacent OH group [36]. The OH of mhpb is observed at 6.05 ppm. Even though there is hydrogen bonding, due to the short range shielding effect induced by neighboring $–OCH_3$, the –OH protons do not shift downfield [37]. Due to the combined resonance and inductive effect of –OH and $–OCH_3$ groups in mhpb, C(9) H is observed as a singlet at 7.72 ppm, and C(12)H and C(13)H are observed as doublets at 7.53 and 6.99 ppm, respectively.

In hpbH, because of intramolecular proton transfer, keto-enol tautomerism exists between –OH and thiazolic N, but in solution enol form predominates. Therefore, the peak at 12.5 ppm is assigned to –OH. The doublets at 7.68 and 7.1 ppm corresponds to C(10)H and C(13)H. The C(12)H is a triplet at 6.94 ppm. The C(11)H resonates at the same frequency as C(6)H, and the corresponding chemical shift is a quartet at 7.39 ppm.

2.5. *Synthesis of the complexes*

To a methanolic solution of $Cu(NO_3)_2 \cdot 3H_2O$ (1 mmol, 0.241 g), a methanolic solution of the corresponding substituted 2-phenylbenzothiazole (2 mmol, 0.482 g, 2-(4-methoxyphenyl)benzothiazole, (mpb); 0.514 g, 2-(3-methoxy-4-hydroxyphenyl) benzothiazole, (mhpb); 0.454 g, 2-(2-hydroxyphenyl)benzothiazole, (hpbH) was added and refluxed for 15 min. To the resulting solution, 1 mL of 10 M HCl was added, which on slow cooling yielded green or yellow crystals suitable for X-ray diffraction. Schematic synthesis of $[(mpbH)_2CuCl_4]$ is given in scheme 2. The same product is obtained with $CuCl_2 \cdot 2H_2O$ under the same conditions but with lower yield.

$(mpbH)_2CuCl_4$: Yield: 90.35%. Color: Dark green. Anal. Found (Calcd for ($C_{28}H_{24}Cl_4CuN_2O_2S_2$, 689.95): C, 48.14 (48.74); H, 3.89 (3.50): N, 4.60 (4.06); S, 9.68 (9.29); Cu, 9.37(9.20).

$(mhpbH)_2CuCl_4$: Yield: 92.35%. Color: Yellow. Anal. Found (Calcd for ($C_{28}H_{24}Cl_4CuN_2O_4S_2$, 721.98):C, 46.11 (46.57); H, 3.90 (3.35): N, 3.58 (3.88); S, 8.20 (8.88); Cu, 8.46 (8.80).

$(hpbH)_2CuCl_4$: Yield: 89.78%. Color: Yellow. Anal. Found (Calcd for ($C_{26}H_{20}Cl_4CuN_2O_2S_2$, 661.93): C, 47.54 (47.17); H, 3.33 (3.04): N, 4.10 (4.23); S, 9.17 (9.68); Cu, 9.87 (9.60).

$$2\,C_{14}H_{11}NOS + Cu^{2+} + 4HCl \xrightarrow[\triangle]{MeOH} (C_{14}H_{12}NOS)_2CuCl_4 + 2H^+$$

Scheme 2. Synthesis of $[(mpbH)_2CuCl_4]$.

3. Results and discussion

The reaction of $Cu(NO_3)_2 \cdot 3H_2O$ with substituted 2-phenylbenzothiazoles and HCl in methanol gave bis(2-(substituted phenyl)benzothiazolium) tetrachlorocuprates. Dark green crystals of $(mpbH)_2CuCl_4$, suitable for X-ray diffraction, crystallized spontaneously from the solution on slow cooling. But $(mhpbH)_2CuCl_4$ and $(hpbH)_2CuCl_4$ precipitated as yellow powders. All were soluble in chloroform and acetonitrile, but decompose in aqueous medium. The Cu(II) in $A_2[CuCl_4]$, is in a distorted tetrahedral coordination environment, which is the common geometry of tetrachlorocuprate anions. The geometry usually varies from distorted tetrahedral with D_{2d} symmetry to centro-symmetric square planar with D_{4h} symmetry. Due to the presence of favorable intermolecular interactions and an active Jahn–Teller effect in Cu(II), the $CuCl_4^{2-}$ species in $(mpbH)_2[CuCl_4]$ has square planar geometry.

3.1. *Crystal structure of $(mpbH)_2CuCl_4$*

The ORTEP view of $(mpbH)_2CuCl_4$ with atom labeling scheme is shown in figure 2. The X-ray crystal data and structure refinement parameters are given in table 1, and selected bond distances and angles are listed in table 2. The crystal data are in agreement with the elemental analysis data of the bulk sample. The unit cell packing of $(mpbH)_2CuCl_4$ is shown in figure 3. The asymmetric unit of the crystal structure features half of $CuCl_4^{2-}$ and one $mpbH^+$. The complete structure can be depicted as encapsulation of discrete $CuCl_4^{2-}$ species in organic layers arranged in zigzag fashion to a 3-D supramolecular network structure (figure 4).

According to the Jahn–Teller theorem, $CuCl_4^{2-}$ deviates from regular tetrahedral geometry. In $(mpbH)_2CuCl_4$, $CuCl_4^{2-}$ has a square planar coordination geometry formed by Cl1, Cl2,

Table 1. Crystal data and structure refinement parameters for $(mpbH)_2CuCl_4$.

Formula weight	689.95
Temperature (K)	293 (2)
Crystal system, space group	Triclinic, $p-1$
Unit cell dimensions	
a (Å)	8.7117(3); $\alpha = 106.280(2)°$
b (Å)	9.5207(3); $\beta = 102.002(2)°$
c (Å)	9.9947(6); $\gamma = 109.152(2)°$
Volume (A^3)	709.39
Z, D_{Calc} (Mg/mm^3)	1,1.615
Absorption coefficient (mm^{-1})	1.3253
F (000)	351
Crystal size (mm)	0.30 × 0.20 × 0.20 mm
θ Range for data collection (°)	2.25–33.42
Limiting indices	$-12 \le h \le 13$, $-14 \le k \le 14$, $-15 \le l \le 15$
Reflections collected/unique [R_{int}]	19,891/5428 [0.0272]
Completeness to $\theta = 30.74$ (%)	99.9
Absorption correction	Semi-empirical from equivalents
Maximum and minimum transmission	0.772 and 0.652
Data/restraints/parameters	5428/1/183
Goodness of fit on F^2	1.039
Final R indices [$I > 2\sigma(I)$]	$R_1 = 0.0368$, $wR_2 = 0.0947$
R indices (all data)	$R_1 = 0.0563$, $wR_2 = 0.1045$
Largest difference in peak and hole (e A^{-3})	0.925 and −0.580

Table 2. Selected bond lengths (Å) and angles (°) for $(mpbH)_2CuCl_4$.

Bond lengths		Bond angles	
C(1)–S(1)	1.7367(18)	C(7)–N(1)–C(6)	115.33(13)
C(6)–N(1)	1.384(2)	C(11)–O(1)–C(14)	118.80(17)
C(7)–N(1)	1.318(2)	C(7)–S(1)–C(1)	91.02(8)
C(7)–C(8)	1.439(2)	Cl(1)–Cu(1)–Cl(1)#1	180.0
C(7)–S(1)	1.7141(15)	Cl(1)–Cu(1)–Cl(2)	90.369(18)
Cl(1)–Cu(1)	2.2374(5)	Cl(1)#1–Cu(1)–Cl(2)	89.631(18)
Cl(2)–Cu(1)	2.2783(5)	Cl(2)–Cu(1)–Cl(2)#1	180.0

Note: Symmetry transformations used to generate equivalent atoms: #1 $-x+1,-y,-z+1$.

Table 3. Hydrogen bond geometry (Å and °) for $(mpbH)_2CuCl_4$.

D–H···A	d(D–H)	d(H···A)	d(D···A)	<(DHA)
C(2)–H(2)···Cl(1)#2	0.93	2.79	3.482(2)	131.9
C(10)–H(10)···O(1)#3	0.93	2.60	3.506(2)	166.3
N(1)–H(1 N)···Cl(1)#4	0.825(9)	2.75(2)	3.2767(15)	123(2)
N(1)–H(1 N)···Cl(2)#5	0.825(9)	2.463(12)	3.2516(14)	160(2)

Note: Symmetry transformations used to generate equivalent atoms: #1 $-x+1, -y, -z+1$; #2 $x, y+1, z$; #3 $-x+2, -y, -z$; #4 $-x+1, -y, -z$; #5 $x, y, z-1$.

Cl1', and Cl2'. This type of distortion is to accommodate a symmetrical structure by multiple non-covalent associations [38, 39].

Discrete unit of $CuCl_4^{2-}$ binds with monomeric $[mpbH]^+$ through hydrogen bonds (table 3) which include asymmetric bifurcated hydrogen bonds [20, 40] lying on either side of the anion, constituting classical hydrogen bonds, N(1)–H(1)···Cl(2) with bond length of N(1)···Cl(2) = 3.2516(14) Å, bond angle N(1)–H(1)···Cl(2) = 160(2)°; and N(1)–H(1)···Cl(1), with bond length of N(1)···Cl(1) = 3.2767(15) Å and a lower bond angle, N(1)–H(1)···Cl(1) = 123(2)°. There exists a non-classical hydrogen bond C9–H9···Cl2, with bond length of C9···Cl2 = 3.689 Å on either side of $CuCl_4^{2-}$ are comparable with tetrachlorocuprate complexes and all these interactions presumably help provide 3-D stability [24, 41]. Bifurcating short contacts N1–Cl1 (3.277 Å) and N1–Cl2 (3.251 Å) originating from thiazolium nitrogen, N1, further stabilize the anion in the cavity. The two trans Cl1 also hold two other $mpbH^+$ units in trans positions by non-classical hydrogen bonds C2-H2···Cl1, with bond length of C(2)···Cl(1) = 3.482(2) Å and by a short contact involving thiazolium S atom, Cl1···S (3.353 Å) [figure 5(a)]. Thus, the crystal architecture is maintained by classical and non-classical hydrogen bonds involving the halogens, and the short contacts [20].

The substituted 2-phenylbenzothiazole is essentially planar. In the thiazole ring of benzothiazole, formed by the condensation of the aldehydic group in anisaldehyde with an amino and thiol of o-aminothiophenol, the C(7)–N(1) bond length of 1.318(2) Å is shorter than the C(1)–S(1) and C(7)–S(1) of 1.7367(18) Å and 1.7141(15) Å in the aromatic system. The other bond lengths are intermediate between ideal values of corresponding single and double bonds giving evidence for extended π-delocalization throughout the entire molecule [42] (figure 2). The orientation of methoxy group is cis to S(1) of the thiazole ring.

Each organic layer contains $mpbH^+$ monomers held together in a zigzag manner by non-classical hydrogen bonds and dihydrogen bonds [43] [figure 5(b)]. The $mpbH^+$ monomer units join end-to-end by parallel non-classical hydrogen bonding of the type C(10)–H(10)···O(1) with C(10)···O(1) bond length of 3.506(2) Å and also by a parallel dihydrogen interaction C(5)–H(5)···H(4)–C(4) with C(5)···C(4) distance of 3.911 Å, arranged in a nearly

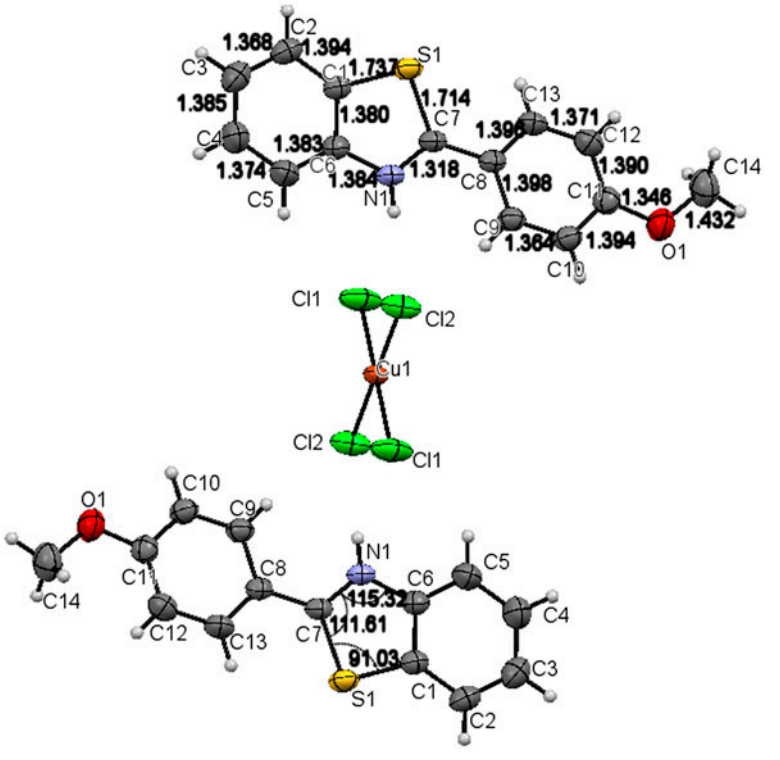

Figure 2. ORTEP diagram of $(mpbH)_2CuCl_4$ showing the atom numbering scheme showing interatomic distances (Å) and important angles (°).

planar supramolecular chain structure. These organic chains, oriented antiparallel, instead of parallel stacking [40], along the b-cell direction as ABAB layers, undergo face-to-face stacked orientation [12, 44, 45] with a $mpbH^+$ centroid–centroid distance of 3.784 Å, which is less than the van der Waal radii of 3.8 Å, forming a supramolecular 3-D structure [figure 5(c)]. Thus, the compound possesses layer structure, with organic cation layers made up of substituted 2-phenyl benzothiazolium and anion layers constituting $CuCl_4^{2-}$, where the anion units are not interconnected by bridging chlorides, Cl···Cl, but in some cases, their interconnection leads to unique properties [13, 15]. These inorganic and organic layers are interconnected by ionic bonds, hydrogen bonds of N–H···Cl type, and the short contacts.

3.2. *Infrared spectra*

The IR spectrum of mpb, mhpb, and hpbH show close similarity with the spectrum of their respective complexes; the spectrum of $[(mpbH)_2CuCl_4]$ compared with the corresponding ligand is shown in figure 6. No significant variation in frequency is noticed for C=N and C–S of benzothiazole moiety and O–CH_3 or OH substituent of phenyl ring in the complexes. Some small changes in intensity/frequency occur due to chemical environment changes of NH^+ after they assemble into 3-D networks. The $\nu_{(C=N)}$ is at 1597–1588 cm^{-1} in all complexes. The $\nu_{(C-S)}$ stretch of thiazole ring appears between

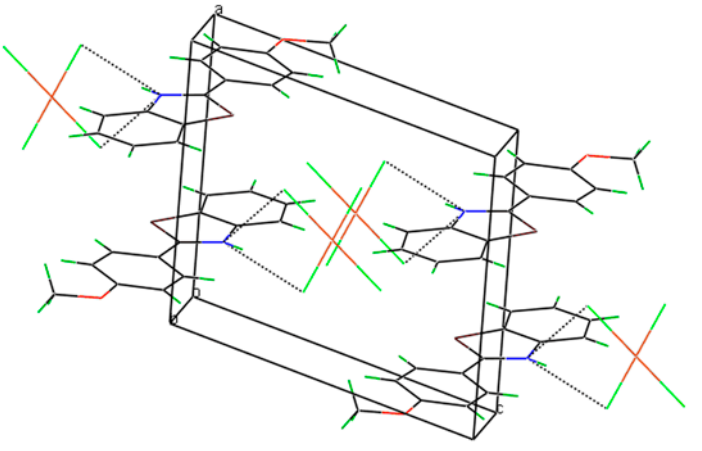

Figure 3. Unit cell packing diagram of $(mpbH)_2CuCl_4$.

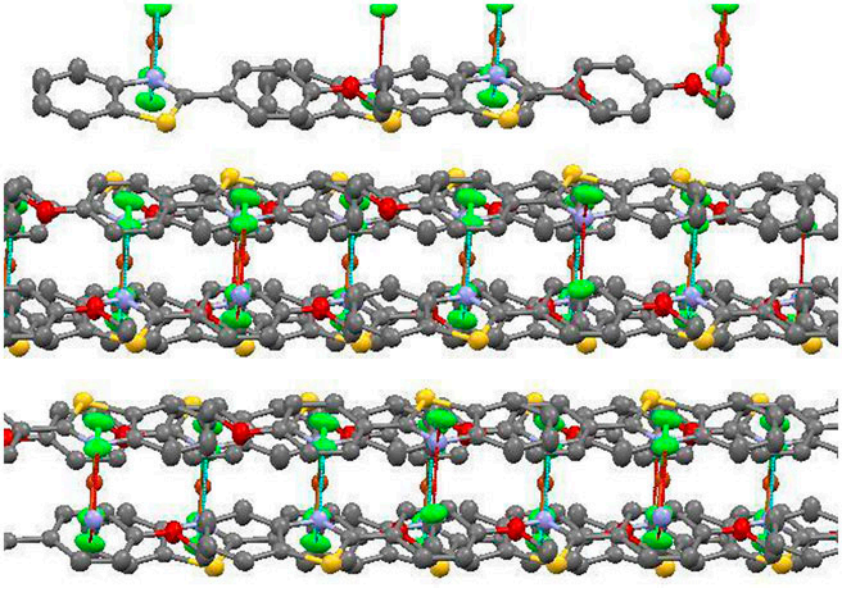

Figure 4. Supramolecular network structure of $(mpbH)_2CuCl_4$. The $CuCl_4^{2-}$ units are encapsulated between antiparallel layers of $mpbH^+$ moieties, which in turn linked by pi–pi stacking interactions.

720 and 685 cm^{-1} in all complexes. These observations suggest non participation of ring N or S in coordination. In the hybrid complexes of mhpb and mpb, O–CH_3 stretching bands are found at 1022–1009 cm^{-1} and bending bands between 440 and 426 cm^{-1}. Bands at 1308–962 cm^{-1} correspond to CH– in plane deformations while out of plane deformations are observed at 860–726 cm^{-1}. These observations indicate that mpb, mhpb, and hpbH do not coordinate with copper. A new broad band between 3400 and 3300 cm^{-1} indicates the presence of N–H, confirming protonation of benzothiazole ring

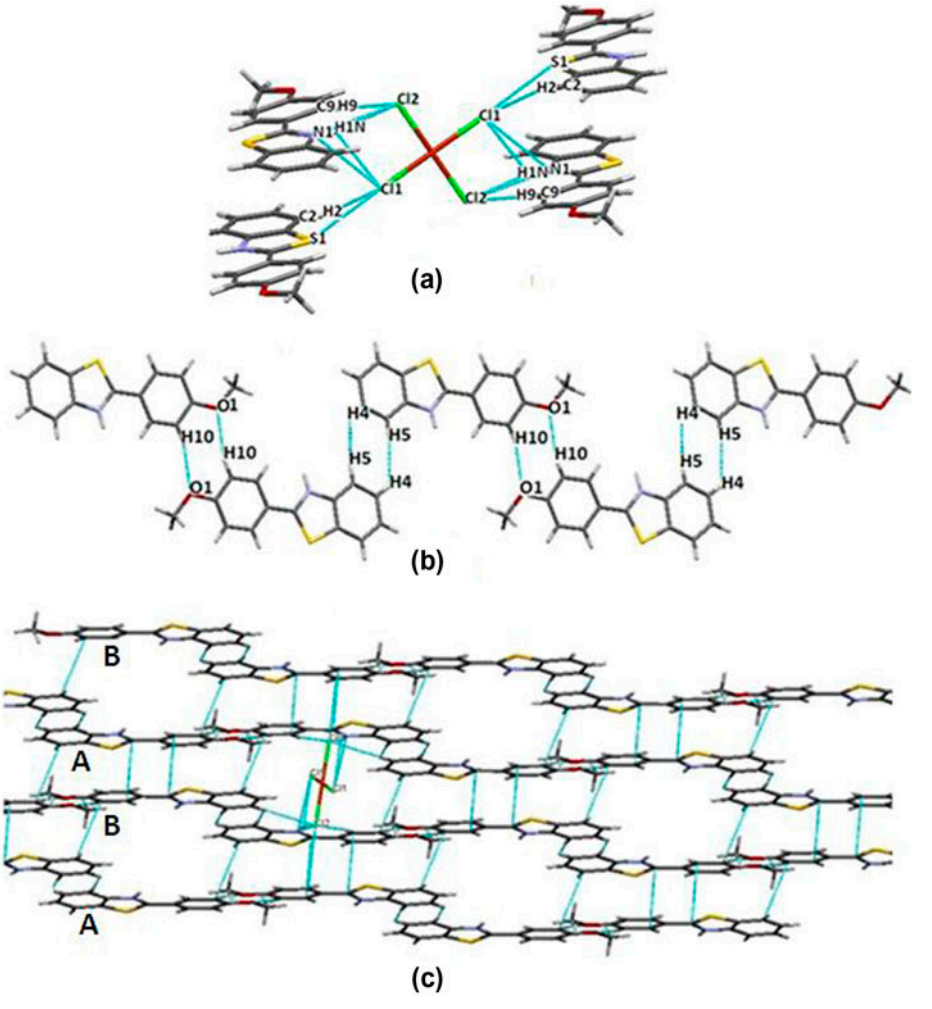

Figure 5. (a) Interactions between $CuCl_4^{2-}$ and $mpbH^+$, (b) Zigzag organic layers connected by short contacts, and (c) Antiparallel cationic ABAB layer structure viewed along the *b* axis.

nitrogen on acidification, thereby forming benzothiazolium cation. For example, in $(mpbH)_2CuCl_4^{2-}$, the IR spectrum of "mpb" does not have a peak at 3000–3500 cm^{-1}, but after complexation, it gives a strong peak around 3400 cm^{-1} due to the asymmetric/symmetric N–H stretching vibration of benzothiazolium salt ($N–H^+$). The $N–H^+$ of benzothiazolium cation subsequently forms hydrogen bonds with Cl^- of MCl_4^{2-} leading to formation of complexes. The broad band around 3400 cm^{-1} also accounts for N–H···Cl hydrogen bonds, the red shift and broadness can be achieved by weakening and subsequent lengthening of the N–H bond by polar nature and by hydrogen bonding [46, 47]. In the case of hpbH and mhpb, very broad bands from 3500 to 2900 cm^{-1} are observed due to overlapping of O–H vibrations with the $N–H^+$ vibrations of thiazolium cation. In accord with the spectral observations, the crystal structure of $(mpbH)_2CuCl_4$ shows the existence of bifurcated hydrogen bonds from $N–H^+$ to Cl^-.

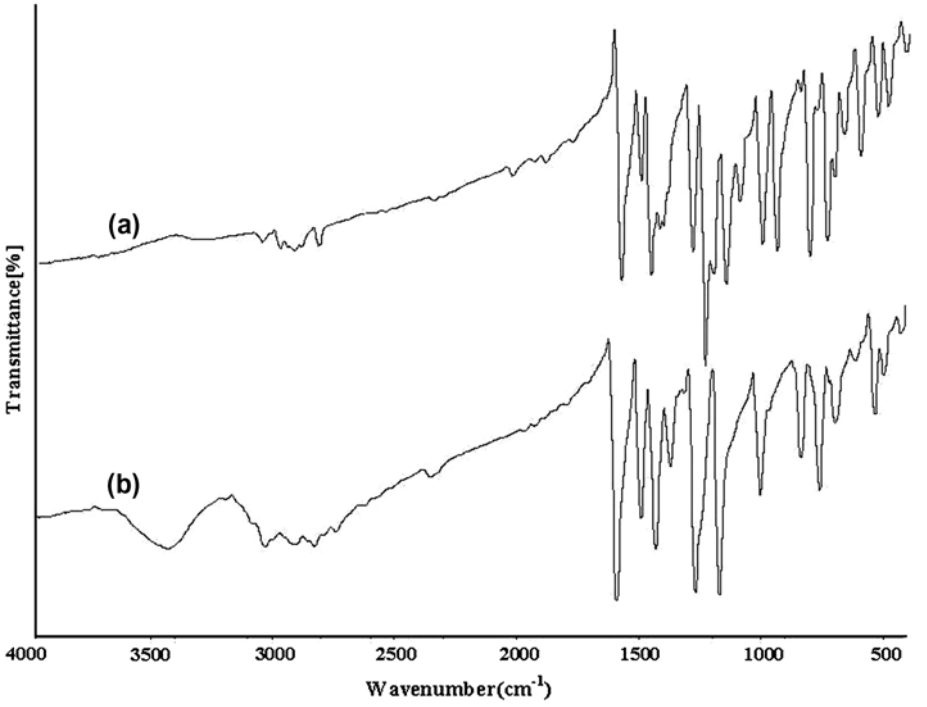

Figure 6. FT-IR spectra of (a) mpb (KBr pellet) and (b) $[(mpbH)_2CuCl_4]$ (KBr pellet).

3.3. *Electronic spectra*

The spectral assignments recorded in acetonitrile are given in table 4. For a square planar Cu(II) complex with a $d_{x^2-y^2}$ ground state, the possible transitions, $d_{x^2-y^2} \rightarrow d_{xy}$, $d_{x^2-y^2} \rightarrow d_{z^2}$ and $d_{x^2-y^2} \rightarrow d_{xz}$, d_{yz} ($^2B_{2g} \leftarrow {}^2B_{1g}, {}^2A_{1g} \leftarrow {}^2B_{1g}$ and $^2E_g \leftarrow {}^2B_{1g}$), cannot be distinguished by their energy as the four d orbitals lie very close together [48]. In conformity with this, the electronic reflectance spectrum of Cu(II) compounds in the solid state, show poorly resolved bands at 580–780 nm, but the electronic spectrum of Cu(II) complexes in acetonitrile, the transitions in high energy region are resolved. Intense transitions in the higher energy region are due to ligand-to-metal and metal-to-ligand charge transfer transitions. Intensities of these transitions are proportional to the overlap of donor and acceptor orbitals involved in charge transfer process. Therefore, strong band around 350 ($\varepsilon = 2576$) nm is assigned as Cl → Cu LMCT transitions [49] and a weak broad band with λ_{max} around 440–476 ($\varepsilon = 407$) nm corresponds to Cu → Cl MLCT and intra-ligand CT transitions. The UV portion of the spectrum is characterized by intense π–π^* transitions of substituted benzothiazole at 256 nm ($\varepsilon = 1806$) and 303 nm ($\varepsilon = 1736$) [50, 51]. The UV portion of the spectrum is characterized by intense π–π^* transitions of substituted benzothiazole ligand.

The dissolution of $(mpbH)_2CuCl_4$ in acetonitrile is also accompanied by a change in the green color of the solid complex to yellow. This may be due to a change in the geometry of solid square planar $CuCl_4^{2-}$, to commonly observed distorted tetrahedral geometry in solution [52]. The appearance of weak peaks at 1030 ($\varepsilon = 385$) nm and 1265 ($\varepsilon = 100$) nm corresponding to $^2B_1 \leftarrow {}^2B_2$, $^2E \leftarrow {}^2B_2$ transitions of D_{2d} geometry support this

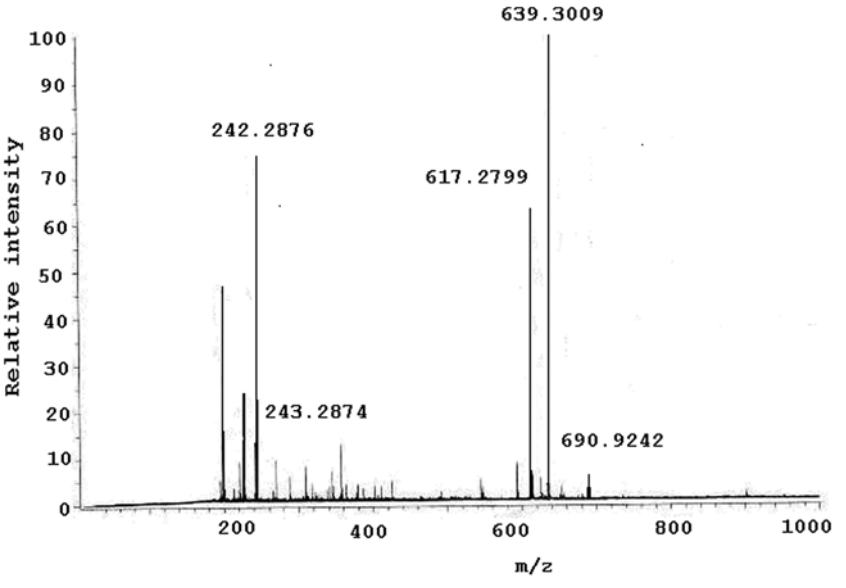

Figure 7. Mass spectrum of $(mpbH)_2CuCl_4$.

Table 4. Electronic spectral assignments (cm^{-1}) of $CuCl_4^{2-}$ complexes of benzothiazoles.

Compounds	$\pi \rightarrow \pi^*$	$n \rightarrow \pi^*$	LMCT	*d–d*
$(mpbH)_2CuCl_4$	255	295	357	1030, 1265
$(mhpbH)_2CuCl_4$	262	291	345	960
$(hpbH_2)_2CuCl_4$	212	286	340	995

observation. Weak d-d bands seen in the near-IR to red part of the visible spectrum around 960 and 995 nm point toward D_{2d} geometry for $[CuCl_4]^{2-}$ in $(mhpbH)_2CuCl_4$ and $(hpbH)_2CuCl_4$.

3.4. *Mass spectral studies*

The mass spectra of the complexes have been recorded in the solid state by DART mass spectrometer using TOF mass analyzer. The analysis was performed in the DART beam of excited helium atoms, which involves predominantly the formation of ionized water cluster followed by proton transfer reaction [53].

The molecular ion peak of $(mpbH)_2CuCl_4$ is observed at *m/z* 690.92 due to $[MH^+]$ with a relative intensity of 5%. The base peak at *m/z* 639.30 is due to $[(M–(CH_3)HCl)H^+]$ (figure 7).

Fragmentation of the complex results in a peak at *m/z* 617.27 due to $[(M–H_2Cl_2)H^+]$ with a relative intensity of 65%. A peak at *m/z* 242.28 with an intensity of 75% is attributed to $[(C_{14}H_{11}NOS)H^+]$ and a less intense peak at *m/z* 243.28 due to $[(C_{14}H_{12}NOS)H^+]$ [54].

Table 5. Thermal decomposition data for $CuCl_4^{2-}$ complexes of benzothiazoles.

Compound	Step	ΔT (°C)	Mass loss % found (Calcd)	Probable species
$(mpbH)_2CuCl_4$	1	20–260	10.65 (10.57)	2HCl
	2	260–348	56.23 (56.45)	$2C_6H_4\text{-}OCH_3 + 2Cl^- + 2C_4H_4$
	3	348–	33.2	
$(mhpbH)_2CuCl_4$	1	20–130	5.13 (5.04)	HCl
	2	130–260	15.15 (15.00)	$HCl + 2Cl^-$
	3	260–330	48.65 (48.40)	$2\{C_6H_3\text{-}OH(OCH_3)\} + C_4H_4$
	4	330–	31.07	
$(hpbH_2)_2CuCl_4$	1	20–270	10.65 (11.01)	2HCl
	2	270–360	55.09 (54.61)	$2C_6H_4\text{-}OH + 2Cl^- + 2C_4H_4$
	3	360–	34.26	

The molecular ion peaks of $(mhpbH)_2CuCl_4$ and $(hpbH)_2CuCl_4$ are observed at *m/z* 722.98 and *m/z* 573.02 due to $[MH^+]$ with a relative intensity of 6 and 8%, respectively. For $(mhpbH)_2CuCl_4$, the base peak at *m/z* 603.4206 is due to $[(M–(OCH_3)HCl(Cl)(OH))H^+]$, and for $(hpbH)_2CuCl_4$, it is at *m/z* 573, due to $[(M–2HCl(OH))H^+]$. A peak at *m/z* 258.16 with an intensity of 66% is attributed to the ligand of $(mhpbH)_2CuCl_4$ while the same for $(hpbH)_2CuCl_4$ is at *m/z* 228 with relative intensity of 58%. These observations of fragments in the mass spectrum support the proposed structures of complexes.

3.5. *TG analysis*

$(mpbH)_2CuCl_4$ exhibits thermochromism, a reversible dependence of color on temperature [55]. In $A_2[MX_4]$ compounds, the thermochromic color change is due to geometry change of $CuCl_4^{2-}$ by heating and is reported that an orange–yellow–green color progression occurs as the anion distortion progresses from tetrahedral to square planar [23, 24]. This change is assisted with a change in hydrogen bonding network pattern that influences the degree of deformation of the metal halogen polyhedron, which is manifested in the change of the absorption spectra [22, 39]. In $(mpbH)_2CuCl_4$, the thermochromic transition is observed at 180 °C, above this temperature the green color changes to yellow, but on cooling, reverts back to green. In the green phase, the $mpbH^+$ units participate in formation of a 3-D network of strong H-bonds that stabilize the square planar coordination of the copper ion, but during thermochromic transition, the N–H···Cl hydrogen bond weakens result in disordering of benzothiazolium cations. This factor increases electrostatic repulsion between chlorides in $CuCl_4^{2-}$ forcing an increased distortion toward tetrahedral geometry. The green-to-yellow thermochromic transition corresponds to a $D_{4h} \rightarrow D_{2d}$ distortion of the $CuCl_4^{2-}$ ion due to a change in its trans Cl–Cu–Cl angle, thereby changing the hydrogen bonding network of the entire crystal [23, 24].

Thermogravimetric experiments in nitrogen at a heating rate of 10 °C min^{-1} were performed to explore the thermal stabilities of the complexes. The thermal decomposition data are given in table 5.

Calculations based on the mass loss confirmed the stoichiometry of two $mpbH^+$/$mhpbH^+$/$hpbH^+$/ units per metal ion in $(mpbH)_2CuCl_4$, $(mhpbH)_2CuCl_4$, and $(hpbH)_2CuCl_4$. Crystal data show that the nitrogen of thiazole ring in mpb is protonated and chloride is present as a counter ion around Cu(II). The first stage of decomposition in $(mpbH)_2CuCl_4$ therefore corresponds to the loss of two hydrogen chloride molecules between 20 and 260 °C. For

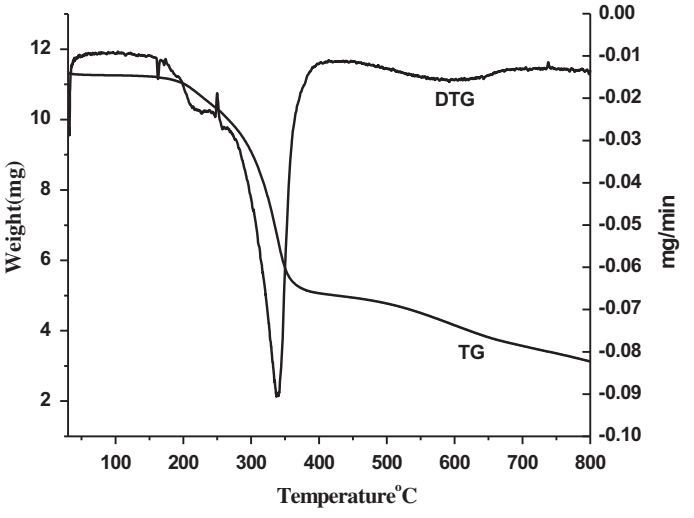

Figure 8. TG and DTG curves of $(mpbH)_2CuCl_4$.

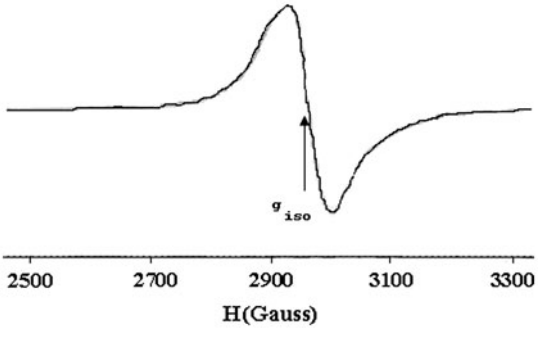

Figure 9. EPR spectrum of $(mpbH)_2CuCl_4$ in polycrystalline state at 298 K.

$(mpbH)_2CuCl_4$, the percentage of hydrogen chloride calculated (10.57%) is in agreement with the value found (10.65%). A mass loss of 56.23% between 260° and 348° corresponds to simultaneous loss of the methoxyphenyl moiety and two chlorides along with partial decomposition of benzothiazole (calculated 56.45%) in a single step. Above 348 °C, the TGA curve shows continuous thermal decomposition and does not stop until heating ends at 800 °C (figure 8). Thermogram of $(mhpbH)_2CuCl_4$ shows four stage decomposition. In the first stage between 20 and 130 °C, the compound loses one HCl, and between 130 and 260 °C, it loses (HCl + 2Cl) followed by loss of $2OCH_3$ and partial decomposition of benzothiazole moiety between 260 and 330 °C. Thereafter, it shows continuous thermal decomposition until heating ends at 800 °C. The first stage decomposition in $(hpbH)_2CuCl_4$ corresponds to loss of two HCl molecules followed by loss of $2Cl^-$ ions and partial loss of benzothiazole moiety corresponding to a mass loss of 55.09% (calculated 54.61%).

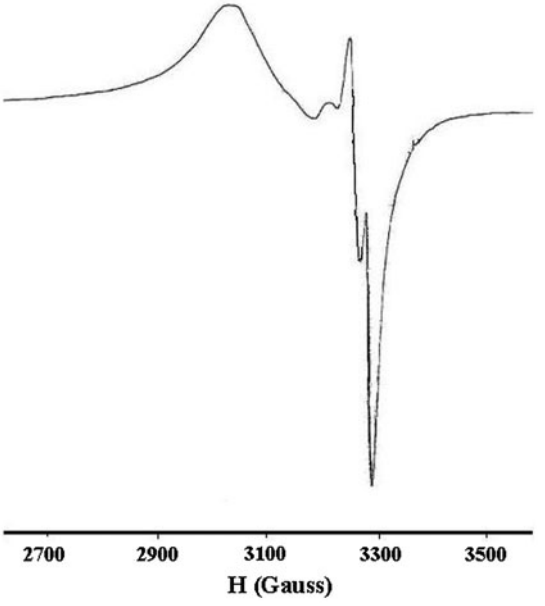

Figure 10. EPR spectrum of $(mpbH)_2CuCl_4$ in frozen acetonitrile at 77 K.

3.6. *EPR spectra*

EPR spectroscopy is a powerful tool to infer the details of complexes formed by paramagnetic metal ions. Cu(II), with a d^9 configuration, has an effective spin of $S = 1/2$ and is associated with a spin angular momentum $m_s = \pm 1/2$, leading to a doubly degenerate spin state in the absence of a magnetic field. In a magnetic field, this degeneracy is lifted and the energy difference between these states is given by $E = h\nu = g\beta H$ where h is the Planck's constant, ν is the frequency, g is Landé splitting factor (equal to 2.0023 for a free electron), β is the Bohr magneton, and H is the magnetic field. The EPR spectra of polycrystalline samples at 298 K and in frozen acetonitrile in 77 K were recorded in the X-band, using 100 kHz field modulation, and g factors were quoted relative to the standard marker TCNE ($g = 2.0023$).

The X-band EPR spectrum of $(mpbH)_2CuCl_4$ (figure 9) and $(mhpbH)_2CuCl_4$ in the polycrystalline state at room temperature shows only one broad signal at $g = 2.189$ and 2.213, respectively, with no absorption at half-field region indicating the existence of a mononuclear species [56]. Such isotropic spectrum, consisting of a broad signal gives no information on the electronic ground state of the Cu(II) ion present in the complex. The spectrum of $(mpbH)_2CuCl_4$ in acetonitrile solution gave non-axial spectra with three g values, $g_1 = 2.23$, $g_2 = 2.08$, and $g_3 = 2.05$, indicating loss of symmetry of the square planar $[CuCl_4]^{2-}$ unit in solution (figure 10). The three g values with $g_1 > g_2 > g_3 > 2.0023$ and $(g_2 - g_3)/(g_1 - g_2) < 1$, suggest a distorted tetrahedral geometry for the complex in solution [57]. $(mhpbH)_2CuCl_4$ in frozen acetonitrile solution at 77 K gave an axial spectrum with well defined $g_{\|}$ and $g_{\perp}$ values of 2.21 and 2.034, respectively, corresponding to values of distorted tetrahedral geometry [14]. Similar observation for $(hpbH)_2CuCl_4$ in solution, $g_{\|} = 2.21$, $g_{\perp} = 2.034$, is also consistent with tetrahedral $[CuCl_4]^{2-}$ [58]. Thus, all Cu(II)

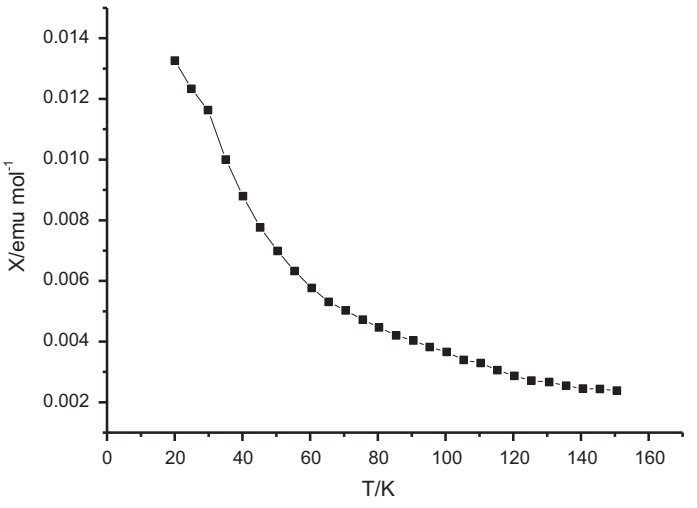

Figure 11. Temperature (T/K) dependences of magnetic susceptibilities (χ/emu mol^{-1}) measured at $H = 4000$ Oe between 20 and 150 K for $(mpbH)_2CuCl_4$.

compounds have D_{2d} geometry in solution. These observations are in agreement with the electronic spectral data and magnetic behavior of the compounds examined.

3.7. *Magnetic properties*

Magnetic susceptibilities (χ) of the compounds were measured on a powdered sample from 20 to 300 K at 4000 Oe with a 7410 Lake Shore vibrating sample magnetometer. The temperature (T/K) dependences of magnetic susceptibilities (χ/emu mol^{-1}) measured at $H = 4000$ Oe between 20 and 150 K for $(mpbH)_2CuCl_4^{2-}$ is shown in figure 11 [14, 59]. The effective magnetic moment (μ_{eff}) values calculated from the equation $\mu_{eff} = 2.828\ (\chi \times T)^{1/2}$ for $(mpbH)_2CuCl_4$ and $(mhpbH)_2CuCl_4$ at room temperature, 1.73 and 1.93 BM, respectively, are normal values for a complex with one unpaired electron. Samples exhibit Curie law behavior from 20 to 150 K, but above this range, there is a deviation from Curie's law. For $(hpbH)_2CuCl_4$, μ_{eff} of 1.65 BM is within experimental error.

3.8. *Electrical conductance*

The solid-state conductivity (σ) of $(mpbH)_2CuCl_4$ at room temperature is 1.99×10^{-4} S cm^{-1} indicating its semi-conducting nature [16]. The value was checked by repeating of the measurements.

4. Conclusion

We report three new ionic complexes of $CuCl_4^{2-}$, with benzothiazolium as cation. They were characterized by X-ray structure analysis, EA, IR, UV, MS, TG, and EPR. The dark green thermochromic crystals, $(mpbH)_2CuCl_4$, spontaneously crystallized during synthesis,

is a semiconducting material at room temperature. All these compounds show paramagnetic behavior. $CuCl_4^{2-}$ displays tetrahedral coordination in $(mhpbH)_2CuCl_4$ and $(hpbH)_2CuCl_4$ while $(mpbH)_2$ $CuCl_4$ is square planar. Multiple non-covalent interactions like bifurcated hydrogen bonds of the type N–H···Cl and weak interactions like C–H···Cl and C–H···O along with π–anion and π–π stacking interactions hold $CuCl_4^{2-}$ and $mpbH^+$ together to maintain the square planar structure of $CuCl_4^{2-}$ in $(mpbH)_2CuCl_4$. These weak bonds are helpful in forming a 3-D supramolecular framework, while stability is attributed by interplay of strong ionic force with weak interactions. All of the compounds show high thermal stabilities.

Supplementary material

Crystallographic data for the structural analysis has been deposited with the Cambridge Crystallographic Data Center, CCDC 809459 for compound [$(mpbH)_2CuCl_4$]. The data can be obtained free of charge at www.ccdc.cam.ac.uk/conts/retrieving.html [or from Cambridge Crystallographic Data Center (CCDC), 12 Union Road, Cambridge CB2 1EZ, UK; fax: +44 0 1223-336033; e-mail: deposit@ccdc.cam.ac.uk].

Acknowledgments

We are grateful to Dr Babu Varghese, SAIF, IIT, Chennai, India, for single crystal X-ray Diffraction studies, IIT Bombay, India, for EPR spectrum and CDRI, Lucknow, India, for DART Mass spectral data.

Disclosure statement

No potential conflict of interest was reported by the authors.

Funding

This work was supported by the University Grants Commission, New Delhi, India.

References

[1] D. Havrylyuk, L. Mosula, B. Zimenkovsky, O. Vasylenko, A. Gzella, R. Lesyk. *Eur. J. Med. Chem.*, **45**, 5012 (2010).
[2] P. Vicini, A. Geronikaki, M. Incerti, B. Busonera, G. Poni, C.A. Cabras, P. La Colla. *Bioorg. Med. Chem.*, **11**, 4785 (2003).
[3] W.P. Hu, Y.K. Chen, C.C. Liao, H.S. Yu, Y.M. Tsai, S.M. Huang, F.Y. Tsai, H.C. Shen, L.S. Chang, J.J. Wang. *Bioorg. Med. Chem.*, **18**, 6197 (2010).
[4] H. Moreno-Díaz, R. Villalobos-Molina, R. Ortiz-Andrade, D. Díaz-Coutiño, J.L. Medina-Franco, S.P. Webster, M. Binnie, S. Estrada-Soto, M. Ibarra-Barajas, I. León-Rivera, G. Navarrete-Vázquez. *Bioorg. Med. Chem.*, **18**, 2871 (2008).
[5] D. Cressier, C. Prouillac, P. Hernandez, C. Amourette, M. Diserbo, C. Lion, G. Rima. *Bioorg. Med. Chem.*, **17**, 5275 (2009).
[6] S.R. Nagarajan, G.A. De Crescenzo, D.P. Getman, H.F. Lu, J.A. Sikorski, J.L. Walker, J.J. McDonald, K.A. Houseman, G.P. Kocan, N. Kishore, P.P. Mehta, C.L. Funkes-Shippy, L. Blystone. *Bioorg. Med. Chem.*, **11**, 4769 (2003).
[7] A. Kamal, K.S. Reddy, M.N.A. Khan, R.V.C.R.N.C. Shetti, M.J. Ramaiah, S.N.C.V.L Pushpavalli, C. Srinivas, M. Pal-Bhadra, M. Chourasia, G.N. Sastry, A. Juvekar, S. Zingde, M. Barkume. *Bioorg. Med. Chem.*, **18**, 4747 (2010).

[8] L. Le Bozec, C.J. Moody. *Aust. J. Chem.*, **62**, 639 (2009).
[9] H. Fu, X. Gao, G. Zhong, Z. Zhong, F. Xiao, B. Shao. *J. Lumin.*, **129**, 1207 (2009).
[10] R. Sarma, B. Nath, A. Ghritlahre, J.B. Baruah. *Spectrochim. Acta, Part A*, **77**, 126 (2010).
[11] S. Tzanopoulou, I.C. Pirmettis, G. Patsis, M. Paravatou-Petsotas, E. Livaniou, M. Papadopoulos, M. Pelecanou. *J. Med. Chem.*, **49**, 5408 (2006).
[12] S. Jin, D. Wang. *J. Coord. Chem.*, **65**, 3188 (2012).
[13] Y. Jin, C. Yu, W. Zhang. *J. Coord. Chem.*, **67**, 1156 (2014).
[14] T.J. Coffey, C.P. Landee, W.T. Robinson, M.M. Turnbull, M. Winn, F.M. Woodward. *Inorg. Chim. Acta*, **303**, 54 (2000).
[15] G.S. Long, M. Wei, R.D. Willett. *Inorg. Chim. Acta*, **36**, 3102 (1997).
[16] D.B. Mitzi, K. Chondroudis, C.R. Kagan. *IBM J. Res. Dev.*, **45**, 29 (2001).
[17] P.R. Hammar, D.C. Dender, D.H. Reich, A.S. Albrecht, C.P. Landee. *J. Appl. Phys.*, **81**, 4615 (1997).
[18] P. Frere, P. Skabara. *Chem. Soc. Rev.*, **34**, 69 (2005).
[19] C.H. Lee, K.W. Lee, C.E. Lee. *Curr. Appl. Phys.*, **3**, 477 (2003).
[20] S.F. Haddad, M.A. AlDamen, R.D. Willett. *Inorg. Chim. Acta*, **359**, 424 (2006).
[21] P. Gamez, G.A. van Albada, L. Mutikainen, U. Turpeinen, J. Reedijk. *Inorg. Chim. Acta*, **358**, 1975 (2005).
[22] M.J. Riley, D. Neill, P.V. Bernhardt, K.A. Byriel, C.H.L. Kennard. *Inorg. Chem.*, **37**, 3635 (1998).
[23] R. Bhattacharya, M. Sinha Ray, R. Dey, L. Righi, G. Bocelli, A. Ghosh. *Polyhedron*, **21**, 2561 (2002).
[24] S. Haddad, R.D. Willett. *Inorg. Chem.*, **40**, 2457 (2001).
[25] B.A. Tuylu, H.S. Zeytinoglu, I. Isikdag. *Biologia (Bratisl.)*, **62**, 626 (2007).
[26] BRUKER, APEX2, SAINT, XPREP, Bruker AXS Inc., Madison, WI (2004).
[27] A. Altomare, G. Cascarano, C. Giacovazzo, A. Guagliardi. *J. Appl. Crystallogr.*, **26**, 343 (1993).
[28] G.M. Sheldrick. *Acta Crystallogr., Sect. A: Found. Crystallogr.*, **64**, 112 (2008).
[29] L.J. Farrugia. *J. Appl. Crystallogr.*, **30**, 565 (1997).
[30] I.J. Bruno, J.C. Cole, P.R. Edgington, M. Kessler, C.F. Macrae, P. McCabe, J. Pearson, R. Taylor. *Acta Crystallogr., Sect. B: Struct. Sci*. 58, 389 (2002).
[31] M. Đaković, H. Čičak, Z. Soldin, V. Tralić-Kulenović. *J. Mol. Struct.*, **938**, 125 (2009).
[32] G. Pavlović, Z. Soldin, Z. Popović, V. Tralić-Kulenović. *Polyhedron*, **26**, 5162 (2007).
[33] R.M. Ramadan, A.M. El-Atrash, A.M.A. Ibrahim. *Spectrochim. Acta, Part A*, **46**, 1305 (1990).
[34] N. Sundaraganesan, K. Sathesh Kumar, C. Meganathan, B. Dominic Joshua. *Spectrochim. Acta, Part A*, **65**, 1186 (2006).
[35] R. Sarma, B. Nath, A. Ghritlahre, J.B. Baruah. *Spectrochim. Acta, Part A*, **77**, 126 (2010).
[36] R.J. Abraham, M. Mobli, R.J. Smith. *Magn. Reson. Chem.*, **41**, 26 (2003).
[37] R.J. Abraham, J.J. Byrne, L. Griffiths, R. Koniotou. *Magn. Reson. Chem.*, **43**, 611 (2005).
[38] S.S. Staniland, A. Harrison, N. Robertson, K.V. Kamenev, S. Parsons. *Inorg. Chem.*, **45**, 5767 (2006).
[39] J. Valdés-Martínez, J.H. Alstrum-Acevedo, R.A. Toscano, S. Hernández-Ortega, G. Espinosa-Pérez, D.X. West, B. Helfrich. *Polyhedron*, **21**, 409 (2002).
[40] R.D. Willett, F. Awwadi, R. Butcher. *Cryst. Growth Des.*, **3**, 301 (2003).
[41] D.H. He, Y.Y. Di, Y. Yao, Y.P. Liu, W.Y. Dan. *J. Chem. Eng. Data*, **55**, 5739 (2010).
[42] P. Sténson. *Acta Chem. Scand.*, **24**, 3729 (1970).
[43] K.N. Robertson, O. Knop. *Can. J. Chem.*, **81**, 727 (2003).
[44] C. Janiak. *J. Chem. Soc., Dalton Trans.*, 3885 (2000).
[45] R.J. Sarma, C. Tamuly, N. Barooah, J.B. Baruah. *J. Mol. Struct.*, **829**, 29 (2007).
[46] J. Joseph, E.D. Jemmis. *J. Am. Chem. Soc.*, **129**, 4620 (2007).
[47] C.L. Nesloney, J.W. Kelly. *J. Org. Chem.*, **61**, 3127 (1996).
[48] A.B.P. Lever. *Inorganic Electronic Spectroscopy*, 2nd edn, Elsevier Science Publishing Company, Amsterdam (1984).
[49] P.F. Rapheal, E. Manoj, M.R. Prathapachandra Kurup. *Polyhedron*, **26**, 818 (2007).
[50] A.M.A. Ibrahim, S.E.D.H. Etaiw. *Polyhedron*, **16**, 1585 (1997).
[51] A. Cerniani, R. Passerini. *J. Chem. Soc.*, 2261 (1954).
[52] K. Thiel, T. Klamroth, P. Strauch, A. Taubert. *Phys. Chem. Chem. Phys.*, **13**, 13537 (2011).
[53] M. Nath, P.K. Saini, G. Eng, X. Song. *J. Organomet. Chem.*, 693, 2271 (2008)
[54] P.E. Sues, A.J. Lough, R.H. Morris. *Organometallics*, **31**, 6589 (2012).
[55] C.F. Zhu. *Thermochim. Acta*, **425**, 7 (2005).
[56] M.J. Bew, B.J. Hathaway, R.J. Fereday. *J. Chem. Soc., Dalton Trans.*, 1229 (1972).
[57] A.S. El-Tabl. *Transition Met. Chem*, **23**, 63 (1998).
[58] A. Wesełucha-Birczyńska, B.J. Oleksyn, S.K. Hoffmann, J. Śliwiński, B. Borzęcka-Prokop, J. Goslar, W. Hilczer. *Inorg. Chem.*, **40**, 4526 (2001).
[59] C.P. Landee, M.M. Turnbull. *J. Coord. Chem.*, **67**, 375 (2014).